



Providing Choice & Value

Generic CT and MRI Contrast Agents



**FRESENIUS
KABI**

CONTACT REP

AJNR

**Whole-Tumor Histogram and Texture
Analyses of DTI for Evaluation of *IDH1*
-Mutation and 1p/19q-Codeletion Status in
World Health Organization Grade II Gliomas**

Y.W. Park, K. Han, S.S. Ahn, Y.S. Choi, J.H. Chang, S.H.
Kim, S.-G. Kang, E.H. Kim and S.-K. Lee

This information is current as
of July 25, 2025.

AJNR Am J Neuroradiol 2018, 39 (4) 693-698

doi: <https://doi.org/10.3174/ajnr.A5569>

<http://www.ajnr.org/content/39/4/693>

Whole-Tumor Histogram and Texture Analyses of DTI for Evaluation of *IDH1*-Mutation and 1p/19q-Codeletion Status in World Health Organization Grade II Gliomas

 Y.W. Park,  K. Han,  S.S. Ahn,  Y.S. Choi,  J.H. Chang,  S.H. Kim,  S.-G. Kang,  E.H. Kim, and  S.-K. Lee



ABSTRACT

BACKGROUND AND PURPOSE: Prediction of the *isocitrate dehydrogenase 1* (*IDH1*)-mutation and 1p/19q-codeletion status of World Health Organization grade II gliomas preoperatively may assist in predicting prognosis and planning treatment strategies. Our aim was to characterize the histogram and texture analyses of apparent diffusion coefficient and fractional anisotropy maps to determine *IDH1*-mutation and 1p/19q-codeletion status in World Health Organization grade II gliomas.

MATERIALS AND METHODS: Ninety-three patients with World Health Organization grade II gliomas with known *IDH1*-mutation and 1p/19q-codeletion status (18 *IDH1* wild-type, 45 *IDH1* mutant and no 1p/19q codeletion, 30 *IDH1*-mutant and 1p/19q codeleted tumors) underwent DTI. ROIs were drawn on every section of the T2-weighted images and transferred to the ADC and the fractional anisotropy maps to derive volume-based data of the entire tumor. Histogram and texture analyses were correlated with the *IDH1*-mutation and 1p/19q-codeletion status. The predictive powers of imaging features for *IDH1* wild-type tumors and 1p/19q-codeletion status in *IDH1*-mutant subgroups were evaluated using the least absolute shrinkage and selection operator.

RESULTS: Various histogram and texture parameters differed significantly according to *IDH1*-mutation and 1p/19q-codeletion status. The skewness and energy of ADC, 10th and 25th percentiles, and correlation of fractional anisotropy were independent predictors of an *IDH1* wild-type in the least absolute shrinkage and selection operator. The area under the receiver operating curve for the prediction model was 0.853. The skewness and cluster shade of ADC, energy, and correlation of fractional anisotropy were independent predictors of a 1p/19q codeletion in *IDH1*-mutant tumors in the least absolute shrinkage and selection operator. The area under the receiver operating curve was 0.807.

CONCLUSIONS: Whole-tumor histogram and texture features of the ADC and fractional anisotropy maps are useful for predicting the *IDH1*-mutation and 1p/19q-codeletion status in World Health Organization grade II gliomas.

ABBREVIATIONS: FA = fractional anisotropy; GLCM = gray level co-occurrence matrices; *IDH* = *isocitrate dehydrogenase*; IDM = inverse different moment; LASSO = least absolute shrinkage and selection operator; WHO = World Health Organization

The World Health Organization (WHO) classification of gliomas was updated in 2016.¹ For the diagnosis of WHO grade II gliomas, the *isocitrate dehydrogenase* (*IDH*)-mutation and 1p/19q-codeletion status are used in combination with the histologic phenotype; the genotype takes precedence over the histologic


phenotype in discordant cases. The molecular subtypes of WHO grade II gliomas are divided into 3 classes: *IDH* wild-type, *IDH* mutant without 1p/19q codeletion, and *IDH* mutant with 1p/19q-codeletion.¹ These molecular subtypes reportedly vary in prognosis and chemosensitivity.² Patients with grade II astrocytomas and *IDH* wild-type have significantly poorer prognoses than those with *IDH*-mutant tumors; the 5-year progression-free survival and overall survival rates are 14% and 51% versus 42% and 93%, respectively.³ Moreover, patients with gliomas with *IDH* mutations were more sensitive to chemoradiation therapy and had longer survival than those with the *IDH* wild-type.⁴ Additionally,


Received October 22, 2017; accepted after revision December 29.

From the Department of Radiology (Y.W.P.), Ewha Womans University College of Medicine, Seoul, Korea; and Departments of Radiology and Research Institute of Radiological Science (Y.W.P., K.H., S.S.A., Y.S.C., S.-K.L.), Neurosurgery (J.H.C., S.-G.K., E.H.K.), and Pathology (S.H.K.), Yonsei University College of Medicine, Seoul, Korea. This work was supported by the Basic Science Research Program through the National Research Foundation of Korea funded by the Ministry of Science, Information and Communication Technologies, and Future Planning (2017R1D1A1B0303440).

Please address correspondence to Sung Soo Ahn, MD, PhD, Department of Radiology and Research Institute of Radiological Science, Yonsei University College of Medicine, 50-one Yonsei-ro, Seodaemun-gu, Seoul 120-752, Korea; e-mail: sung-soo@yuhs.ac.

 Indicates open access to non-subscribers at www.ajnr.org.

 Indicates article with supplemental on-line tables.

 Indicates article with supplemental on-line photos.

<http://dx.doi.org/10.3174/ajnr.A5569>

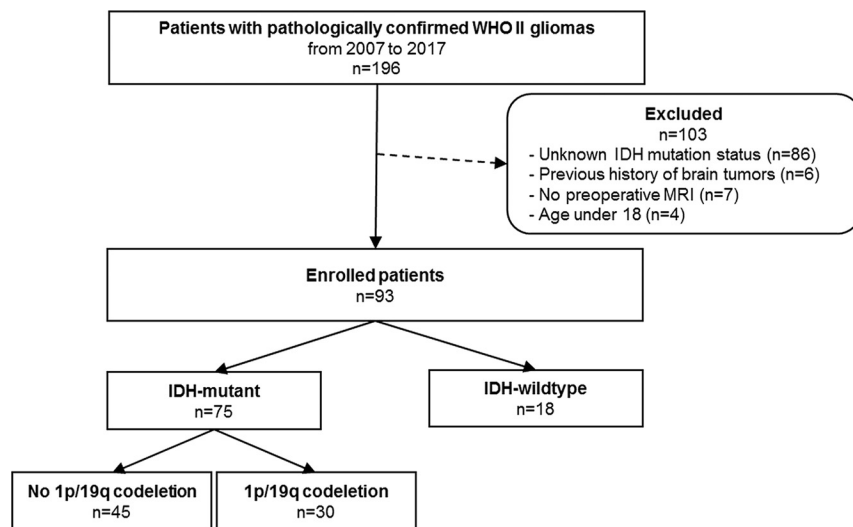


FIGURE. Flowchart of the study population.

1p/19q codeletion predicts therapeutic response and survival.⁵ Thus, predicting the *IDH*-mutation and 1p/19q-codeletion status of WHO grade II gliomas preoperatively may aid in predicting prognosis and planning treatment strategies.

IDH mutation and 1p/19 codeletion may reflect alterations in tumor cell proliferation and microvessel density that exhibit characteristic features on ADC and fractional anisotropy (FA) parameters. The ADC is an index of tumor cellularity, reflecting tumor burden and correlating negatively with glioma grade.^{1,6} DTI provides information about the motion of water protons at the cellular level⁷; the directional restriction of water diffusivity can be measured as the FA, which correlates with myelinated fiber tract integrity.^{8,9} ADC and FA histograms may predict histologic subtypes, such as oligodendroglioma, oligoastrocytoma, and astrocytoma in WHO grade II gliomas.^{10,11} However, these studies did not obtain molecular markers, and mean or histogram percentile values of ADC and FA have limitations in terms of evaluation of gliomas, due to the heterogeneity.¹² Histogram-based measures can reflect the intensity distribution of a volume of interest, but not the spatial distribution of these intensities.¹³ On the other hand, texture analysis features show the characteristics of the entire tumor and allow noninvasive quantification of tumor features, such as tumor uniformity, heterogeneity, smoothness, randomness, and symmetry.¹⁴

To the best of our knowledge, there have been no previous reports that have comprehensively examined the whole-tumor histogram and texture features (ie, ADC and FA parameters), according to the *IDH*-mutation and 1p/19q-codeletion status of grade II gliomas. This study evaluated the role of histogram and texture analyses of ADC and FA maps based on the entire tumor volume in determining the *IDH*-mutation and 1p/19q-codeletion status of grade II gliomas, preoperatively.

MATERIALS AND METHODS

Patient Population

The institutional review board waived the need for obtaining informed patient consent for this retrospective study. Between January 2007 and February 2017, one hundred ninety-six patients

with pathologically diagnosed WHO grade II gliomas were included in this study. Inclusion criteria were as follows: 1) WHO grade II gliomas confirmed by histopathology; and 2) patients who underwent preoperative MR imaging, including DTI, with a b-value of 600 s/mm². Exclusion criteria were the following: 1) an unknown *IDH1*-mutation status ($n = 86$), 2) patients with a previous history of brain tumor ($n = 6$), 3) patients with incomplete MR imaging sequences or suboptimal images ($n = 7$), and 4) patients younger than 18 years of age ($n = 4$). The flow chart of the study population is shown in the Figure. The mean interval between the MR imaging examination and the operation was 10.73 ± 12.49 days.

Immunohistochemical analysis and peptide nucleic acid-mediated clamping polymerase chain reaction were performed to detect the *IDH1* R132H mutation.¹⁵ For immunohistochemistry, monoclonal antibody H09 was used, and the degree of *IDH1*-R132H staining was determined as positive in patients with any stained cells or as negative in those without any stained cells.¹⁶ If immunohistochemistry results were negative for *IDH1*-R132H, we confirmed the *IDH1* status by peptide nucleic acid-mediated clamping polymerase chain reaction. Fluorescence in situ hybridization analysis was used to investigate 1p/19q codeletion.¹⁷

MR Imaging Protocol

Preoperative MR imaging was performed with a 3T MR imaging scanner (Achieva; Philips Healthcare, Best, the Netherlands) with an 8-channel sensitivity encoding head coil. The preoperative MR imaging protocol included T1-weighted (TR/TE, 1800–2000/10–15 ms; FOV, 240 mm; section thickness, 5 mm; matrix, 256×256), T2-weighted (TR/TE, 2800–3000/80–100 ms; FOV, 240 mm; section thickness, 5 mm; matrix, 256×256), and FLAIR (TR/TE, 9000–10,000/110–125 ms; FOV, 240 mm; section thickness, 5 mm; matrix, 256×256) sequences. 3D contrast-enhanced T1-weighted images (TR/TE, 6.3–8.3/3.1–4 ms; FOV, 240 mm; section thickness, 1 mm; matrix, 192×192) were acquired after administering 0.1 mL/kg of gadolinium-based contrast material (gadobutrol, Gadovist; Bayer Schering Pharma, Berlin, Germany). Whole-brain DTI was performed with b-values of 600 and 0 s/mm², 32 directions, and the following parameters: TR/TE, 8413.4/77 ms; FOV, 220 mm; section thickness, 2 mm; matrix, 112×112 ; acceleration factor, 2.5; and with an acquisition time of 5 minutes 20 seconds.

Image Postprocessing: Volume Acquisition

DTI data were processed off-line with the Medical Image Processing, Analysis, and Visualization software package, Version 7.0 (National Institutes of Health; <https://mipav.cit.nih.gov/>). T2-weighted images were coregistered to ADC and FA maps using affine transformation with normalized mutual information as a cost function,^{18,19} and the ROIs were drawn on every tumor

Table 1: Patient characteristics according to the *IDH1*-mutation status and 1p/19q-codeletion status^a

	<i>IDH1</i> Wild-Type (<i>n</i> = 18)	<i>IDH1</i> Mutant without 1p/19q Codeletion (<i>n</i> = 45)	<i>IDH1</i> Mutant with 1p/19q Codeletion (<i>n</i> = 30)
Age (yr) (mean)	49.57 ± 3.45	40.80 ± 1.25	45.10 ± 1.91
Sex			
Male	8 (44.4)	27 (60)	13 (43.3)
Female	10 (55.6)	18 (40)	17 (56.7)
Karnofsky performance status (mean)	88.89 ± 1.37	90.67 ± 1.12	91.00 ± 1.39
Extent of resection			
Gross total resection	7 (38.9)	29 (64.5)	15 (50)
Subtotal/partial resection	7 (38.9)	14 (31.1)	14 (46.7)
Biopsy	4 (22.2)	2 (4.4)	1 (3.3)

^a Unless otherwise indicated, data are presented as number of patients (%).

section on T2-weighted images using a semiautomatic method, with signal intensity thresholds as previously described.²⁰ The ROIs, were drawn by a single neuroradiologist (Y.W.P) and confirmed by another neuroradiologist (S.S.A.) and were transferred to ADC and FA maps.

Histogram and Texture Analysis of ADC and FA

First-Order Statistics Including Histogram Parameters. ADC and FA histogram parameters consisting of the mean value and SD were calculated from ROIs overlaid on ADC and FA maps. For cumulative ADC and FA histograms, the 10th, 25th, 50th, 75th, and 90th percentile ADC and FA values in the histogram were generated.¹⁰ Skewness and kurtosis were also calculated.

Second-Order Statistics via Gray Level Co-Occurrence Matrices. Texture analysis via gray level co-occurrence matrices (GLCM) allows extraction of second-order statistical texture features from images.²¹ Co-occurrence matrix texture considers the relationship between 2 pixels, the reference and neighboring pixel, reflecting local heterogeneity. We used the following parameters for quantitative analysis of the summation of 2D ROIs: contrast, dissimilarity, inverse different moment 1 (IDM1), homogeneity or IDM2, energy, maximum probability, entropy, mean, variance, SD, correlation, cluster shade, and cluster prominence in ADC and FA maps. Altogether, ADC and FA map features were quantified by various features, including their degrees of uniformity (IDM1, homogeneity [IDM2], angular second moment, and energy), heterogeneity (contrast, dissimilarity, variance, and SD), smoothness (correlation), randomness (entropy), and symmetry (cluster shade and prominence). To obtain rotational invariant features, we computed the co-occurrence matrix by averaging >4 uniformly distributed angular directions (0°, 45°, 90°, and 135°).

Statistical Analysis

The differences between ADC and FA histogram parameters and *IDH1*-mutation status were assessed using the Student *t* test or the Mann-Whitney *U* test, according to normality test results. Because the number of significant imaging features was relatively large, compared with the number of patients when comparing the *IDH1* wild-type and *IDH1*-mutant groups, we used the regularization method to assess the predictive power of the imaging features based on the least absolute shrinkage and selection operator (LASSO), which reduces the potential risk of overfitting or false discovery. LASSO involves penaliz-

Table 2: Prediction model for an *IDH1*-mutation status in WHO grade II gliomas using the LASSO procedure

Imaging Parameters	Adjusted OR for <i>IDH1</i> Wild-Type
ADC skewness	1.04
ADC energy	1.15
FA 10th percentile	23.19
FA 25th percentile	998.91
FA correlation	0.004

ing irrelevant variables to zero and retains only useful features, thereby effectively reducing the number of variables. We used 5-fold cross-validation to find the optimal regularization parameter for LASSO. We estimated the area under the receiver operating curve to assess the predictive ability of variables by selecting significant variables based on LASSO. The 5-fold cross-validated area under the receiver operating curve is the average of the predictive areas under the receiver operating characteristic curve of 5 validation datasets generated by the cross-validation process.

The identical process was performed to evaluate correlations between ADC and FA histograms and 1p/19q-codeletion status in the *IDH1*-mutant subgroup.

Statistical analysis was performed using R statistical and computing software (Version 3.3.1; <http://www.r-project.org/>). Statistical significance was set at *P* < .05.

RESULTS

The characteristics of the 93 enrolled patients with WHO grade II gliomas are summarized in Table 1. Eighteen patients had *IDH1* wild-type tumors, 45 had *IDH1*-mutant without 1p/19q-codeletion tumors, and 30 had *IDH1*-mutant with 1p/19q-codeletion tumors.

Histogram and Texture Analyses of ADC and FA Values for Determining *IDH1*-Mutation Status

Various histogram and texture analyses features differed significantly between the *IDH1* wild-type and *IDH1*-mutant groups (On-line Table 1). Among these factors, 5 were independently associated with predicting the *IDH1* mutation based on the LASSO procedure (Table 2). The *IDH1* wild-type group had higher skewness and energy of ADC and FA 10th and 25th percentiles, whereas the *IDH1*-mutant group had a higher FA correlation. The area under the receiver operating curve for the optimal model was 0.853 (95% confidence interval, 0.761–0.945).

Table 3: Prediction model for 1p/19q-codeletion status in *IDH1*-mutant WHO grade II gliomas using the LASSO procedure

Imaging Parameters	Adjusted OR for 1p/19q Codeletion
ADC skewness	1.71
ADC cluster shade	1.00
FA energy	0.005
FA correlation	0.12

Histogram and Texture Analyses of ADC and FA Values for Determining 1p/19q-Codeletion Status in the *IDH1*-Mutant Group

Various histogram and texture analysis features were significantly different according to the 1p/19q-codeletion status in the *IDH1*-mutant subgroup (On-line Table 2). Among these factors, 4 were independently associated with predicting the 1p/19q-codeletion status on the basis of the LASSO procedure (Table 3). The 1p/19q-codeletion group had higher ADC skewness and cluster shade, whereas the group without 1p/19q codeletion had higher FA energy and FA correlation. The area under the receiver operating curve for the optimal model was 0.807 (95% confidence interval, 0.649–0.965). Representative cases according to *IDH1*-mutation and 1p/19q-codeletion status are demonstrated in On-line Fig 1. On-line Fig 2 shows the heat map according to *IDH1*-mutation and 1p/19q-codeletion status, which reveals the strong relationship between significant histogram and texture features of ADC and FA maps ($P < .05$) and molecular subtypes.

DISCUSSION

WHO grade II gliomas are heterogeneous at both genetic and histopathologic levels, with intratumoral spatial variation²²; we comprehensively analyzed the histogram and texture features of whole tumors using ADC and FA maps according to the molecular subtypes.

ADC and FA histogram analyses differ significantly according to histopathologic subtypes or molecular markers of WHO grade II/III gliomas.^{10,23,24} However, some study groups followed the 2007 WHO classification, and texture analyses have not been performed in all studies. Spatial textures in the ADC and FA signals arise from destruction of normal anatomy by tumors, vasogenic edema, tumor cellularity, degenerative changes, or the compression of normal structures, including some that are imperceptible to human eyes. The notion that texture analysis can reveal visually imperceptible tumor information extends beyond radiology to histopathology; texture analysis (in conjunction with histopathology) has been reported to be more accurate than histopathology alone in predicting prognosis in malignant gliomas.²⁵ In WHO grade II gliomas, *IDH* wild-type tumors showed lower ADC and higher FA values than *IDH1*-mutant tumors, in agreement with our results.^{11,23,26} Generally, increased tumor cell proliferation and angiogenesis increase tumor cellularity,²⁷ and the diffusivity of water molecules is restricted in environments with high cellular density, resulting in lower ADCs.²⁸ Therefore, this finding suggests that *IDH* mutation is associated with lower tumor cellularity²⁹ and explains why the presence of an *IDH* mutation is a favorable prognostic marker in patients with glioma.²

DTI-based FA values have received attention in the detection of glioma infiltration.³⁰ Previous studies have suggested that tu-

mors with higher FA values have higher tumor cell density and a relatively high Ki-67 index in malignant brain tumors, which indicate greater malignancy potential.^{30,31} Therefore, the mechanisms underlying lower FAs in WHO grade II gliomas with *IDH* mutations may involve a lower rate of proliferation and aggressiveness and lower tumor cell densities of these tumors. In our study, various ADC and FA histograms and texture features differed statistically significantly according to *IDH1*-mutation status; this finding is useful for enhancing the understanding of tumor heterogeneity according to *IDH1*-mutation status. The *IDH1* wild-type group had higher skewness and energy of ADC and 10th and 25th percentiles of FA, whereas the *IDH1*-mutant group demonstrated higher FA correlation. The energy represents the orderliness of the image; when the image is highly organized, the energy values are high. Correlation is a measure of the linear dependence of gray levels on those of neighboring pixels (ie, local gray-level dependence); higher values can be obtained for similar gray-level regions. Thus, the *IDH1* wild-type group demonstrated higher ADC orderliness, whereas the *IDH1*-mutant group had a higher frequency of similar FA value regions. Few studies have analyzed the texture features of T1 contrast-enhanced or T2 FLAIR images according to the *IDH1*-mutation status of WHO grade II gliomas^{32,33}; but none performed DTI analyses, which provide insight into the spatial distribution of the tumor cellularity and myelinated fiber tract integrity.

In a recent study, diffusion characteristics from visual assessment were significantly different according to the 1p/19q-codeletion status in *IDH1*-mutant grade II gliomas.³⁴ For further evaluation of the roles of diffusion characteristics in determining the 1p/19q-codeletion status of WHO grade II gliomas, we evaluated histogram and texture features measured quantitatively, which can be more objective. Our results demonstrate that histogram and texture features can be effective for predicting 1p/19q-codeletion status. The 1p/19q-codeletion group demonstrated higher ADC skewness, whereas the 1p/19q-intact group had higher FA energy and FA correlation. Thus, the 1p/19q-codeletion group showed more ADC asymmetry, whereas the 1p/19q-intact group had higher FA organization and more regions with similar FA values. Previous studies showed discrepant results of association between 1p/19q codeletion and ADC and/or FA features in WHO grade II gliomas,^{24,26,35,36} which may be due to different study groups, smaller sample sizes, and different imaging analyses. Several studies included oligoastrocytic or oligodendroglial tumors based on histopathology, according to the 2007 WHO classification, regardless of *IDH*-mutation status; then the authors classified them according to 1p/19q codeletion status. Therefore, a small number of patients with *IDH* wild-type gliomas might have been included. Additionally, previous studies included fewer WHO grade II gliomas with evaluation of focal ROIs of the tumor instead of the entire tumor volume.

Because WHO grade II glioma is a heterogeneous tumor with cystic or calcified areas, ADC or FA values calculated in small ROIs cannot represent the cellular density or arrangement of the whole tumor. However, we analyzed tumors according to 1p/19q-codeletion status in an *IDH1*-mutant subgroup throughout the whole tumor volume, using comprehensive texture analyses. *IDH1*-mutant with 1p/19q-codeletion tumors showed lower

ADC and higher FA values than *IDH1*-mutant without 1p/19q-codeletion tumors. *IDH*-mutant with 1p/19q-codeletion tumors are markedly infiltrated by perineuronal satellitosis, with more persistent neurons, as seen on pathology, which may explain their higher FA values.¹¹ If the neurons are spared and the volume of invasion is less, edema should be less, which may explain the lower ADC values in such tumors.¹¹ Calcification is another pathologic finding related to differences in ADC and FA values according to the 1p/19q-codeletion status in *IDH1*-mutant tumors; microcalcifications are seen in up to 90% of *IDH*-mutant with 1p/19q codeletion tumors.¹¹ Tumors with calcifications are expected to have lower ADC values, due to lack of water movement in the calcified region.

Our study had several limitations. First, it was based on a single-center, retrospectively collected dataset. Second, prognostic markers were not analyzed because patients with WHO II gliomas have a relatively long overall survival. Further studies are needed to correlate prognostic markers, such as overall survival and progression-free survival with genotypic and imaging features. Third, $b = 600 \text{ s/mm}^2$ was used instead of $b = 1000 \text{ s/mm}^2$ or higher in DTI. This low b -value may have resulted in overestimation of ADC values due to perfusion effects. However, this would have little effect on analyzing the difference between molecular groups because the pixels as a whole are affected. Fourth, only *IDH1* R132H mutation was detected in our hospital, and a small proportion of *IDH2*-mutation or non-*IDH1* R132H mutation tumors was not detected. However, it has been previously reported that the predominant amino acid sequence alteration in *IDH1* mutation is R132H, accounting for 92.7% of the detected mutations in WHO grade II and III gliomas.³⁷ Fifth, this retrospective study did not investigate the direct relationship between ADC and tumor cellularity from histologic specimens. However, previous studies have proved the negative correlation between ADC and tumor cellularity.^{38,39}

CONCLUSIONS

Histogram and texture features of ADC and FA maps of the entire tumor volume differ according to the *IDH1*-mutation and 1p/19q-codeletion status in WHO grade II gliomas and may be helpful for predicting molecular status.

Disclosures: Sung Soo Ahn—RELATED: Grant: This research received funding from the Basic Science Research Program through the National Research Foundation of Korea funded by the Ministry of Science, Information and Communication Technologies, and Future Planning (2017R1D1A1B03030440). * *Money paid to the institution.

REFERENCES

- Louis DN, Perry A, Reifenberger G, et al. The 2016 World Health Organization classification of tumors of the central nervous system: a summary. *Acta Neuropathol* 2016;131:803–20 CrossRef Medline
- Brat DJ, Verhaak RG, Aldape KD, et al; Genome Atlas Research Network. Comprehensive, integrative genomic analysis of diffuse low-grade gliomas. *N Engl J Med* 2015;372:2481–98 CrossRef Medline
- Metellus P, Coulibaly B, Colin C, et al. Absence of *IDH* mutation identifies a novel radiologic and molecular subtype of WHO grade II gliomas with dismal prognosis. *Acta Neuropathol* 2010;120:719–29 CrossRef Medline
- Olar A, Wani KM, Alfaro-Munoz KD, et al. *IDH* mutation status and role of WHO grade and mitotic index in overall survival in grade II–III diffuse gliomas. *Acta Neuropathol* 2015;129:585–96 CrossRef Medline
- Jenkins RB, Blair H, Ballman KV, et al. A t (1; 19)(q10; p10) mediates the combined deletions of 1p and 19q and predicts a better prognosis of patients with oligodendroglioma. *Cancer Res* 2006;66:9852–61 CrossRef Medline
- Omuro A, DeAngelis LM. Glioblastoma and other malignant gliomas: a clinical review. *JAMA* 2013;310:1842–50 CrossRef Medline
- Balss J, Meyer J, Mueller W, et al. Analysis of the *IDH1* codon 132 mutation in brain tumors. *Acta Neuropathol* 2008;116:597–602 CrossRef Medline
- Chenevert TL, Brunberg JA, Pipe JG. Anisotropic diffusion in human white matter: demonstration with MR techniques in vivo. *Radiology* 1990;177:401–05 CrossRef Medline
- Hansen JR. Pulsed NMR study of water mobility in muscle and brain tissue. *Biochim Biophys Acta* 1971;230:482–86 CrossRef Medline
- Tozer DJ, Jäger HR, Danchaivijitr N, et al. Apparent diffusion coefficient histograms may predict low-grade glioma subtype. *NMR Biomed* 2007;20:49–57 CrossRef Medline
- Khayal IS, McKnight TR, McGue C, et al. Apparent diffusion coefficient and fractional anisotropy of newly diagnosed grade II gliomas. *NMR Biomed* 2009;22:449–55 CrossRef Medline
- Ryu YJ, Choi SH, Park SJ, et al. Glioma: application of whole-tumor texture analysis of diffusion-weighted imaging for the evaluation of tumor heterogeneity. *PLoS One* 2014;9:e108335 CrossRef Medline
- Brynnförs P, Nilsson D, Henriksson R, et al. ADC texture: an imaging biomarker for high-grade glioma? *Medical Phys* 2014;41:101903 CrossRef Medline
- Davnull F, Yip CS, Ljungqvist G, et al. Assessment of tumor heterogeneity: an emerging imaging tool for clinical practice? *Insights Imaging* 2012;3:573–89 CrossRef Medline
- Yan H, Parsons DW, Jin G, et al. *IDH1* and *IDH2* mutations in gliomas. *N Engl J Med* 2009;360:765–73 CrossRef Medline
- Takano S, Tian W, Matsuda M, et al. Detection of *IDH1* mutation in human gliomas: comparison of immunohistochemistry and sequencing. *Brain Tumor Pathol* 2011;28:115–23 CrossRef Medline
- Riemenschneider MJ, Jeuken JW, Wesseling P, et al. Molecular diagnostics of gliomas: state of the art. *Acta Neuropathol* 2010;120:567–84 CrossRef Medline
- Cha J, Kim S, Kim HJ, et al. Differentiation of tumor progression from pseudoprogression in patients with posttreatment glioblastoma using multiparametric histogram analysis. *AJNR Am J Neuroradiol* 2014;35:1309–17 CrossRef Medline
- Maes F, Collignon A, Vandermeulen D, et al. Multimodality image registration by maximization of mutual information. *IEEE Trans Med Imaging* 1997;16:187–98 CrossRef Medline
- Ko SB, Choi HA, Carpenter AM, et al. Quantitative analysis of hemorrhage volume for predicting delayed cerebral ischemia after subarachnoid hemorrhage. *Stroke* 2011;42:669–74 CrossRef Medline
- Haralick RM, Shanmugam K. Textural features for image classification. *IEEE Trans Syst Man Cybern* 1973;610–21 CrossRef
- Paulus W, Peiffer J. Intratumoral histologic heterogeneity of gliomas: a quantitative study. *Cancer* 1989;64:442–47 Medline
- Xiong J, Tan WL, Pan JW, et al. Detecting isocitrate dehydrogenase gene mutations in oligodendroglial tumors using diffusion tensor imaging metrics and their correlations with proliferation and microvascular density. *J Magn Reson Imaging* 2016;43:45–54 CrossRef Medline
- Jenkinson MD, Smith TS, Brodbelt AR, et al. Apparent diffusion coefficients in oligodendroglial tumors characterized by genotype. *J Magn Reson Imaging* 2007;26:1405–12 CrossRef Medline
- Zacharaki EI, Morita N, Bhatt P, et al. Survival analysis of patients with high-grade gliomas based on data mining of imaging variables. *AJNR Am J Neuroradiol* 2012;33:1065–71 CrossRef Medline
- Xiong J, Tan W, Wen J, et al. Combination of diffusion tensor imaging and conventional MRI correlates with isocitrate dehydrogenase 1/2 mutations but not 1p/19q genotyping in oligodendroglial tumours. *Eur Radiol* 2016;26:1705–15 CrossRef Medline

27. Fischer I, Gagner JP, Law M, et al. **Angiogenesis in gliomas: biology and molecular pathophysiology.** *Brain Pathol* 2005;15:297–310 [Medline](#)
28. Yamasaki F, Kurisu K, Satoh K, et al. **Apparent diffusion coefficient of human brain tumors at MR imaging.** *Radiology* 2005;235:985–91 [CrossRef Medline](#)
29. Bralten LB, Kloosterhof NK, Balvers R, et al. **IDH1 R132H decreases proliferation of glioma cell lines in vitro and in vivo.** *Ann Neurol* 2011;69:455–63 [CrossRef Medline](#)
30. Beppu T, Inoue T, Shibata Y, et al. **Fractional anisotropy value by diffusion tensor magnetic resonance imaging as a predictor of cell density and proliferation activity of glioblastomas.** *Surg Neurol* 2005;63:56–61; discussion 61 [CrossRef Medline](#)
31. Kinoshita M, Hashimoto N, Goto T, et al. **Fractional anisotropy and tumor cell density of the tumor core show positive correlation in diffusion tensor magnetic resonance imaging of malignant brain tumors.** *Neuroimage* 2008;43:29–35 [CrossRef Medline](#)
32. Yu J, Shi Z, Lian Y, et al. **Noninvasive IDH1 mutation estimation based on a quantitative radiomics approach for grade II glioma.** *Eur Radiol* 2017;27:3509–22 [CrossRef Medline](#)
33. Li Z, Wang Y, Yu J, et al. **Deep learning based radiomics (DLR) and its usage in noninvasive IDH1 prediction for low grade glioma.** *Sci Rep* 2017;7:5467 [CrossRef Medline](#)
34. Leu K, Ott GA, Lai A, et al. **Perfusion and diffusion MRI signatures in histologic and genetic subtypes of WHO grade II-III diffuse gliomas.** *J Neurooncol* 2017;134:177–88 [CrossRef Medline](#)
35. Khayal IS, Vandenberg SR, Smith KJ, et al. **MRI apparent diffusion coefficient reflects histopathologic subtype, axonal disruption, and tumor fraction in diffuse-type grade II gliomas.** *Neuro Oncol* 2011;13:1192–201 [CrossRef Medline](#)
36. Park Y, Han K, Ahn S, et al. **Prediction of IDH1-mutation and 1p/19q-codeletion status using preoperative MR imaging phenotypes in lower grade gliomas.** *AJNR Am J Neuroradiol* 2018;39:37–42 [CrossRef Medline](#)
37. Hartmann C, Meyer J, Balss J, et al. **Type and frequency of IDH1 and IDH2 mutations are related to astrocytic and oligodendroglial differentiation and age: a study of 1,010 diffuse gliomas.** *Acta Neuropathol* 2009;118:469–74 [CrossRef Medline](#)
38. Kono K, Inoue Y, Nakayama K, et al. **The role of diffusion-weighted imaging in patients with brain tumors.** *AJNR Am J Neuroradiol* 2001;22:1081–88 [Medline](#)
39. Sugahara T, Korogi Y, Kochi M, et al. **Usefulness of diffusion-weighted MRI with echo-planar technique in the evaluation of cellularity in gliomas.** *J Magn Reson Imaging* 1999;9:53–60 [Medline](#)